

---

# Experimental investigation of the oil jet heat transfer on meshing spur gears

Emre Ayan, Christian Kromer, Corina Schwitzke, Hans-Jörg Bauer  
emre.ayan@kit.edu

Karlsruhe Institute of Technology  
Institute of Thermal Turbomachinery  
Karlsruhe  
Germany

## ABSTRACT

Designing an adequate cooling system for a high-speed high-power gearbox of a geared turbofan requires a thorough understanding of the cooling capabilities of the utilized oil jet impingement. An experimental setup is employed to determine the heat transfer coefficient on gear teeth in various non-meshing and meshing configurations, which incorporate inclined jets with varying distances between the impingement and the meshing zones. The direction of heat transfer is inverted in the experiments to allow for a feasible setup with the rotating gears, where impinging oil jets heat the hollow instrumented gear as its inner surface is cooled via air jet impingement. Measurements with varying oil volume flow rates and rotational speeds are carried out. The losses are analyzed to enable an isolated investigation of the heat transfer between the oil and the gear via measured temperatures on the gear teeth. Heat transfer coefficients are compared at the lower rotational speed with relatively small meshing losses. The meshing in the experimental setup does not have a significant influence on the mean heat transfer coefficient. The spatial distribution of the heat transfer coefficient is slightly affected by the meshing teeth as the distribution gets more uniform with decreasing distance between the impingement and meshing zones.

**Keywords:** geared turbofan; heat transfer; oil jet impingement

## NOMENCLATURE

AF	active flank
BL	bottom land
$d_n$	nozzle diameter
$E$	nozzle outlet eccentricity
$h$ , HTC	heat transfer coefficient
$h^*$	relative local heat transfer coefficient
$\Delta \bar{h}_{\%}$	deviation of mean heat transfer coefficient from base configuration
$\Delta \bar{h}_{\text{brake}}$	deviation of mean heat transfer coefficient from no-load configuration
$L$	length of the path across one tooth
$l_n$	nozzle length
$m$	tooth module
$n_n$	number of nozzles
$P_{\text{bearing,spin}}$	load-independent bearing losses
$P_{\text{bearing,load}}$	load-dependent bearing losses
$P_{\text{brake}}$	braking power
$P_{\text{mv}}$	oil deflection and acceleration or momentum variation losses
$P_{\text{friction}}$	friction losses
$P_{\text{spin}}$	load-independent or spin losses
$P_{\text{load}}$	load-dependent losses
$P_{\text{loss}}$	total losses
$P_{\text{trapping}}$	trapping losses
$P_{\text{windage}}$	windage losses
PF	passive flank
$\dot{q}$	heat flux
$R^2$	coefficient of determination
$R_{\text{corr}}$	correlation factor
$r_{\text{p,g}}$	geometrical pitch radius
$r_{\text{p,w}}$	working pitch radius
$r_r$	root radius
$r_{\text{spraybar}}$	spray bar axis offset
$r_t$	tip radius
$s$	circumferential coordinate
$s^+$	dimensionless circumferential coordinate
$T_{\text{oil}}$	oil temperature
$T_{\text{TC}}$	thermocouple temperature
TL	top land
$u_{\text{jet,t}}$	tangential speed of the oil jet
$u_{\text{p,g}}$	circumferential speed of the gear at $r_{\text{p,g}}$
$\dot{V}_{\text{oil}}$	oil volume flow rate
$W$	gear width
$x$	profile shift
$y$	axial coordinate
$y^+$	dimensionless axial coordinate

## Greek Symbol

$\alpha_n$	jet inclination
$\theta_m$	base positional angle
$\theta_v$	operational positional angle
$\rho_{\text{oil}}$	oil density
$\sigma$	standard deviation
$\omega$	rotational speed

## 1.0 INTRODUCTION

Installing a gearbox between the fan and the low-pressure spool enables both components to operate at optimal speeds. As with each component of an aero-engine, the gearbox needs to be highly efficient and reliable. Ensuring both the efficiency and the reliability of such a gearbox requires a detailed understanding of the relevant aspects that affect the power transmission itself and the wear of the gears. Various loss mechanisms such as friction, windage, and lubricant trapping lead to heat dissipation within the gearbox, increasing gear and lubricant temperatures. The increased temperature lowers the lubricant's viscosity and increases the risk of a failure of the lubrication film. This, in turn, would culminate in ever-increasing gear and lubricant temperatures and finally in a total failure of the gearbox. The gears should therefore be continuously cooled using an adequate cooling strategy.

The standard approach for cooling such high-speed high-power gearboxes is oil jet impingement cooling. However, its heat transfer characteristics are not thoroughly investigated in the literature. Either empirical functions for rotating bodies [11, 5] or the fling-off cooling model of DeWinter and Blok [4] are employed in thermal modeling of the gearbox to account for the cooling of gear teeth [17, 21, 12]. Most of the studies [21, 19, 10, 8, 3] use loaded gear pairs, which hinders defining clear boundary conditions required to characterize the heat transfer experimentally. Von Plehwe et al. [22] developed and employed an experimental method that allows for an isolated investigation of the heat transfer on a single gear impinged upon by oil jets. This method is based on an iterative evaluation approach to determine the heat transfer coefficient (HTC) on a hollow and rotating gear utilizing discrete temperature measurements. Ayan et al. [2] implemented a new iterative method in the evaluation approach and validated it using reference studies. This work aims to modify the existing experimental setup of von Plehwe et al. [22] and use the evaluation approach of Ayan et al. [2] to investigate the influence of meshing on the cooling characteristics of the inclined impingement cooling.

## 2.0 EXPERIMENTAL SETUP

The experimental setup at the Institute of Thermal Turbomachinery is designed to induce a temperature gradient over the radius of a hollow and rotating gear made out of TiAl6V4 (depicted in black in Figure 1). This temperature gradient allows for heat transfer coefficient determination on the gear teeth. The direction of the gradient is inverted for the experimental setup. The impinging oil (depicted in orange in Figure 1) is at a higher temperature than the instrumented gear, which is cooled via air jets (depicted in blue in Figure 1) impinging upon its inner surface. Inverting the heat transfer direction makes a setup, where the measured temperatures on the rotating gear are to be transmitted wirelessly, feasible. The wireless transmission is carried out via a telemetry system. Temperature is acquired via 21 thermocouples of type K on the gear: 18 on the surface of the teeth and 3 on the inner surface. The gear is impinged upon at one circumferential position by four identical cylindrical jets equidistantly distributed over the gear width. All jets are expected to induce identical heat transfer distributions on each tooth quarter. The heat transfer on both halves of the cylindrical jets should also be symmetrical. Therefore, all thermocouples are located axially on one-eighth of the gear (Figure 2). The thermocouples are placed on different teeth to make the instrumentation possible. The evaluation of the measurements is carried out in a time-averaged manner, where the time-dependent differences between different teeth are not relevant. A transformation into the so-called tooth coordinate system (Figure 2) is required to evaluate the measurements [2]. The axial coordinate  $y$  is normalized with the total axial width  $W$  of the gear ( $y^+ = y/W$ ), and the circumferential coordinate  $s$  is normalized analogously with the path length along one tooth  $L$  ( $s^+ = s/L$ ). The oil temperature is measured via a thermocouple mounted within the so-called spray bar. This thermocouple is of type K in all measurements except C2 configurations (Figure 3), where a thermocouple of type T with a higher accuracy replaces the broken thermocouple.

The experimental setup of von Plehwe et al. [22] is modified to enable measurements with meshing gears. A second, geometrically similar yet non-instrumented and uncooled



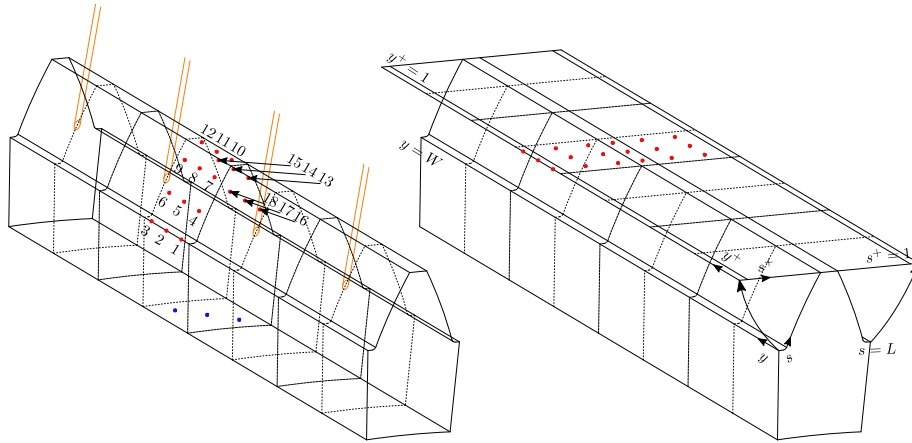


Figure 2: Instrumentation of the gear depicted on one tooth with the oil jets in orange, the thermocouples on the tooth surface in red with corresponding thermocouple number, and the thermocouples on the air-cooled surface in blue. The transformation into the tooth coordinate system is shown on the right [2].

tion means that the tangential velocity component of the jet and the circumferential velocity of the impinged gear are pointed in the same direction. The oil temperature in the spray bar  $T_{oil}$  is kept at  $80^\circ \pm 1.5^\circ$  C. Some operational parameters are varied within this study to assess their influence on the measured differences between various configurations. These variable parameters are the oil volume flow rate  $\dot{V}_{oil}$ , varied in three steps of {3.2, 3.66, 4.4} l/min, and the rotational speed  $\omega$ , varied in three steps of {2000, 3000, 4000} RPM.

The investigated configurations are depicted in Figure 3. The naming convention of the configurations is CXY, where C stands for configuration, X stands for an arbitrary number to differentiate between possible configurations, and Y stands for the rotational direction of the instrumented gear. Y can be either L, meaning the instrumented gear is rotating counterclockwise, or R, meaning the rotational direction of the instrumented gear is clockwise. COL is the only configuration without meshing and is also called the base configuration within this work. The base configuration is used as a benchmark to assess the influence of meshing on the inclined impingement setup. The mean heat transfer coefficient of the meshing configurations, averaged over the tooth surface, will be presented relative to the mean HTC of the base configuration in the following. C1R is the configuration, where the spray bar is located in its base position, and the instrumented gear is rotating clockwise. The distance traveled by a tooth between the impingement and meshing zones is at its maximum. With the assumption that the distance between the impingement point and the first contact between the gears can be approximated with the positional angle of the spray bar, the freshly impinged upon tooth completes 91.4% of a rotation before reaching the meshing zone. The influence of meshing on the measured HTC is a priori expected to be at its minimum since the spreading of the oil film and the oil volume decrease via fling-off process -therefore also the heat transfer between the oil and the gear- are progressed further than other configurations, if not finalised completely [9]. The configuration C1L is the other extreme case, where the spray bar is located at its base position, and the instrumented gear rotates counterclockwise. The impingement occurs shortly before the tooth enters the meshing zone in this configuration. The tooth completes only 8.6% of its rotation before reaching the pitch point. Since there is less time for the spreading and fling-off processes before meshing, the expectation is to observe the maximum influence on the measured HTC. C2R and C2L are two cases between both extremes, where the tooth completes 63.1% and 36.9% of a rotation, respectively, before reaching the pitch point. Nine operating points are measured for each configuration with a full factorial design, where the volume flow and rotational speed are the variables.

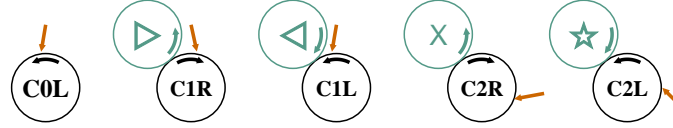


Figure 3: Configurations investigated within this work. The black circle depicts the instrumented gear, and the green circle the non-instrumented gear. The arrows within the circles show the rotational direction of the respective gear. The orange arrow is the oil jet. The names within the black circles are the names of the configurations. The symbols within the green circles are the markers in the results section for the corresponding configuration.

### 3.0 LOSS ANALYSIS

The determination of HTC is based on an iterative evaluation of the measured temperatures. For the non-meshing configuration C0L, the oil temperature in the spray bar and temperatures on the gear can be utilized to calculate the HTC ( $h$ ) using

$$\dot{q} = h(T_{\text{oil}} - T_{\text{TC}}), \quad \dots (1)$$

where  $\dot{q}$  is the normal heat flux, and  $T_{\text{TC}}$  is the temperature measured by a thermocouple [2, 22]. However, meshing introduces additional heat sources into the energy balance in the form of meshing losses. These lead to a temperature increase on the tooth surface and a misrepresentation of the HTC if not accounted for during the evaluation. Losses are analyzed to quantify these meshing losses.

The total losses  $P_{\text{loss}}$  in the test rig can be described by

$$P_{\text{loss}} = P_{\text{load}} + P_{\text{spin}}, \quad \dots (2)$$

with the load-dependent losses  $P_{\text{load}}$  and the load-independent or spin losses  $P_{\text{spin}}$ . The load-dependent losses can be broken down into friction losses of the meshing teeth  $P_{\text{friction}}$  and loaded bearing losses  $P_{\text{bearing,load}}$ . The spin losses comprise the load-independent bearing losses  $P_{\text{bearing,spin}}$ , the windage losses  $P_{\text{windage}}$ , the oil deflection and acceleration or momentum variation losses  $P_{\text{mv}}$ , and the oil and air trapping (pocketing, squeezing) losses  $P_{\text{trapping}}$  [16]. Other loss sources such as seal rubbing or auxiliary systems are negligible.

The non-meshing configuration has no output drive, meaning the driving power  $P_{\text{COL}}$  is equal to the power losses in the test rig, and load-dependent losses, as well as trapping losses, are non-existent:

$$P_{\text{COL}} = P_{\text{loss}} = P_{\text{windage}} + P_{\text{mv}} + P_{\text{bearing,spin}}. \quad \dots (3)$$

It is first investigated whether installing a brake on the output drive to simulate a small load leads to any differences in the measured temperatures and HTCs with meshing configuration C1L. A hysteresis brake with up to 200 W of continuous braking power is utilized for the measurements with loaded gears. Multiple operating points are measured with braking powers  $P_{\text{brake}}$  of 0 W, 100 W, and 200 W. An effect on the measured temperatures is not observed. No correlation between the HTCs and braking power is found after evaluating the measurements (Figure 4). The brake also does not lead to any improvement regarding the operation of the test rig. Therefore, remaining meshing measurements are carried out without utilizing the brake, eliminating the load-dependent losses from Equation 2:

$$P_{\text{C1,C2}} = P_{\text{loss}} = P_{\text{windage}} + P_{\text{mv}} + P_{\text{trapping}} + P_{\text{bearing,spin}}. \quad \dots (4)$$

A series of measurements is carried out to quantify the windage and bearing losses. The first measurement setup consists of the instrumented gear and air impingement on the inside. The oil jet is rotated away from the gear to rotate the gear in an atmosphere with oil mist while eliminating the oil momentum variation losses. The rotational speed is varied between 500 RPM and 4000 RPM. Measurements are carried out with both counterclockwise and clockwise rotations. The second setup includes the non-instrumented gear without air cooling, and experiments are analogous to the first setup. The results are

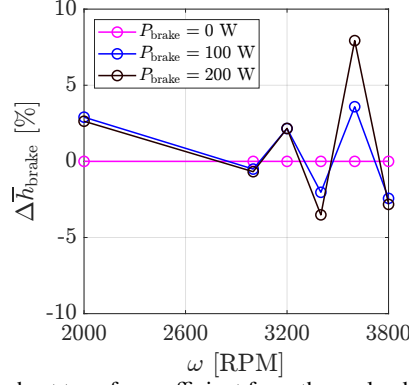


Figure 4: Deviation of mean heat transfer coefficient from the no-load case with  $\Delta \bar{h}_{\text{brake}} = (\bar{h}_{P_{\text{brake}}} / \bar{h}_{P_{\text{brake}}=0}) - 1$ . The measurements are carried out with C1L and  $\dot{V}_{\text{oil}} = 3.6$  l/min.

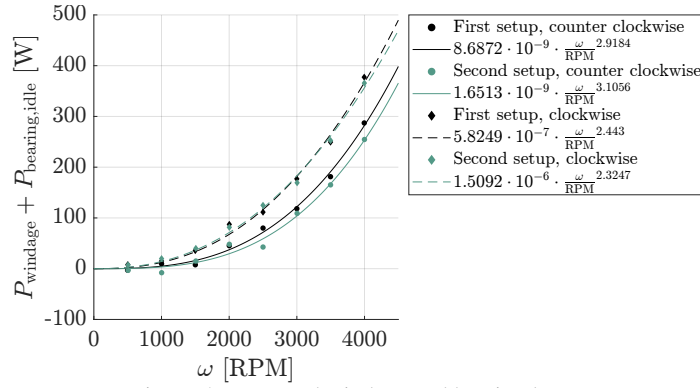


Figure 5: Measured windage and bearing losses

shown in Figure 5 with fitting functions in the form of  $f(\omega) = C_1 \frac{\omega}{\text{RPM}}^{C_2}$ , utilizing the least-squares method.

Similarly to [1, 6, 13], momentum variation losses are calculated using

$$P_{\text{mv}} = (u_{\text{p,g}} - u_{\text{jet,t}}) \rho_{\text{oil}} \dot{V}_{\text{oil}} r_{\text{p,g}} \omega, \quad \dots (5)$$

with the circumferential speed of the gear at the geometrical pitch radius  $u_{\text{p,g}}$ , tangential speed of the oil jet  $u_{\text{jet,t}}$  and the oil density  $\rho_{\text{oil}}$  at  $T_{\text{oil}}$ .

The validity of the loss calculations is evaluated by comparing the driving powers of various COL measurements with the calculated losses using Equation 3. Figure 6 compares the measured and calculated losses of 247 operating points, where apart from the variables within this study, jet inclination, nozzle numbers, nozzle diameters, and nozzle lengths are also varied. The calculated losses are in excellent agreement with the measured losses, resulting in a high coefficient of determination  $R^2 = 0.984$  and a low standard deviation of  $\sigma = 2.59\%$ .

The same loss calculation approach is used for meshing configurations, assuming that a superposition of individual windage and bearing losses is valid\*. Recently, Ruzek et al. [18] showed that the total windage loss of a gear pair is equal to or less than that of two individual gears. Since the rotational speeds of the gears in the test rig are below the critical threshold given by Ruzek et al. [18], the total windage loss is calculated by adding up the individual components. The total bearing losses are also assumed to be equal to the sum of individual bearing losses, since the bearings used for both drives are the same. The trapping losses are determined by subtracting the calculated loss components from the driving power. For example, the windage and bearing losses for configuration C1R are assumed to be the addition of the losses of the instrumented gear with clockwise rotation

\* Ideally, the windage and bearing losses would be measured with a meshing setup and without oil impingement. However, the metal-to-metal contact could lead to additional losses and, more importantly, create the risk of gear or, at the very least, thermocouple damage and failure.

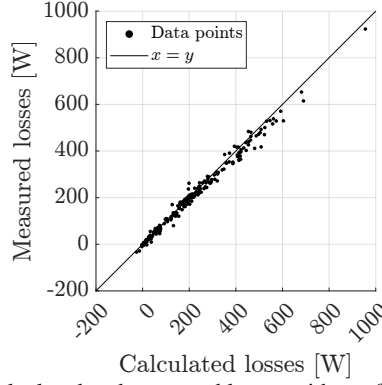
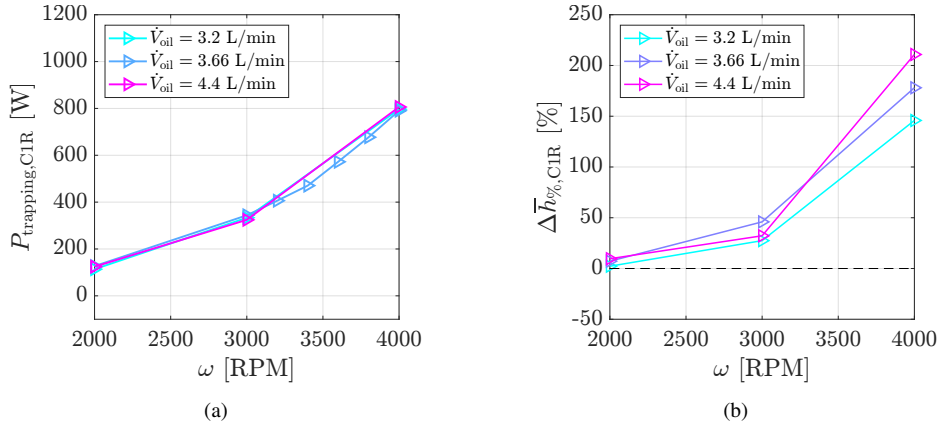


Figure 6: Calculated and measured losses with configuration C0L

Figure 7: Trapping losses (a) and HTC deviation  $\Delta\bar{h}_{\%}$  (b) for configuration C1R.

and the non-instrumented gear with counterclockwise rotation as in Figure 5. For C1L, the rotational directions are reversed. The calculated trapping losses for C1R are depicted in Figure 7a. The trapping losses correlate strongly with the rotational speed, whereas the oil volume flow rate does not significantly affect them. These observations are in accordance with Fondelli et al. [7] and Massini et al. [14], respectively.

## 4.0 RESULTS

As mentioned before, the influence of meshing on the HTC for inclined cooling, in either positive or negative direction, is expected to be in the ascending order for C1R, C2R, C2L, and C1L. In order to assess this influence, the deviation of the mean HTC of a meshing configuration  $i$  from the mean HTC of C0L is formulated by means of

$$\Delta\bar{h}_{\%,i} = \frac{\bar{h}_i}{\bar{h}_{C0L}} - 1, \quad i \in \{C1R, C1L, C2R, C2L\}. \quad \dots (6)$$

Even for C1R, a significant deviation from the mean HTC of C0L is observed except for the measurements at lower rotational speeds of 2000 RPM (Figure 7b). The trapping losses correlate strongly with the observed deviation in HTC (correlation factor of  $R_{\text{corr}} = 0.9685$ ), hinting at an influence of trapping losses on the measured temperatures. Correcting this influence is challenging since critical questions such as where the heat dissipation occurs, whether the heat is dissipated into oil, air, or the gears, and how much oil is present on the gear tooth during the meshing can not be answered clearly. Therefore, the results presented in the following will be focusing only on measurements with 2000 RPM, where the trapping losses are relatively small, and the deviation of C1R from C0L is less than 10%.

Figure 8 shows the  $\Delta\bar{h}_{\%}$  values for C1 and C2 configurations over the measured volume flow rates at the rotational speed of 2000 RPM. All measurements except two with C2R result in higher mean HTC's compared to the base configuration COL. This deviation from COL could be related to the trapping losses. Eliminating the additional heat input by trapping losses would decrease the temperatures on the gear and, therefore, decrease the determined HTC. The expected ascending order of C1R, C2R, C2L, and C1L is not observed. The maximum difference between both a priori defined extremes, C1R and C1L, is 14% at the volume flow rate of  $\dot{V}_{oil} = 4.4$  l/min. Configurations with the same rotational direction tend to result in similar mean HTC's, with  $\bar{h}$  of counterclockwise rotating configurations higher than those with clockwise rotation. The rotational direction change means that, e.g., the active flank is measured with one set of thermocouples in C1L (4 to 9 in Figure 2) and another set of thermocouples in C1R (13 to 18 in Figure 2). The systematic inaccuracies of the thermocouples could lead to the observed differences in mean HTC's. The negative deviations with C2R can also be explained with the difference in rotational directions of C2R and COL. Further measurements with a new configuration, C0R, where the non-meshing gear rotates in clockwise rotation, could clarify how the HTC is related to the rotational direction. The influence of meshing on mean HTC's is classified as insignificant at 2000 RPM, since

- the maximum deviation from COL is at 24% with C1L, and expected to decrease if the influence of trapping losses are eliminated,
- the maximum deviation between both extremes, C1L and C1R, is at 14%, and expected to decrease if the influence of rotational direction is eliminated,
- no clear effect of the distance between the impingement and meshing zones is observed.

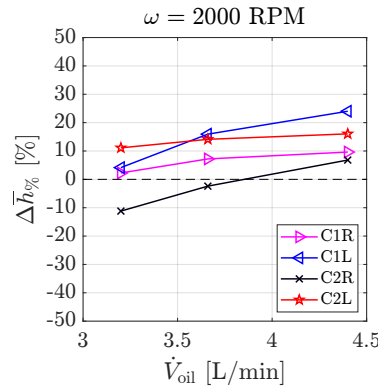


Figure 8:  $\Delta\bar{h}_{\%}$  for configurations C1R, C1L, C2R and C2L at 2000 RPM

The so-called heat transfer maps of one-quarter of the tooth surface, e.g., for a case with COL in Figure 9, can be utilized to assess the influence of meshing on the spatial distribution of heat transfer. The local HTC is depicted dimensionless as the ratio of the HTC at an arbitrary location to the mean HTC determined for the respective operating point with

$$h^* = \frac{h}{\bar{h}}. \quad \dots(7)$$

The coordinates in the heat transfer maps are given in the so-called tooth coordinate system, where the  $y^+$  direction is the dimensionless axial coordinate and  $s^+$  is the dimensionless circumferential coordinate. The white vertical lines indicate the borders between different regions of the tooth, such as the bottom land (BL), the active flank (AF), the top land (TL), and the passive flank (PF). The  $s^+$  coordinate starts at the middle of one bottom land and ends at the middle of the next one. It should be noted that the  $s^+$  coordinate is inverted in clockwise rotating configurations, e.g., in Figure 10a. The reason for the inversion is to enable a visual comparison of two cases with different rotational directions so that the active flank is always on the left side and the passive flank is always on the right side of a figure.

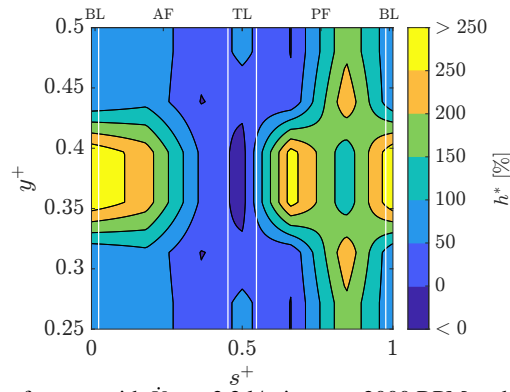


Figure 9: Heat transfer map with  $\dot{V}_{oil} = 3.2$  l/min,  $\omega = 2000$  RPM and configuration COL.

The heat transfer map of an operating point with  $\dot{V}_{oil} = 3.2$  l/min,  $\omega = 2000$  RPM, and base configuration COL is depicted in Figure 9. High levels of HTC are present at both the active and passive flanks of the tooth, which is expected for this operating point since the high jet velocity and relatively low rotational speed of the gear result in the tangential component of the jet velocity exceeding the circumferential velocity of the gear tooth. Therefore, the oil jet is able to reach the passive flank of the tooth and contributes to a continuous impingement from one top land to the next one. The heat transfer maps present comparable distributions for C1R and C2R as depicted in Figures 10a and 10c with a relatively narrow region of high heat transfer on the active flank and axially uniform distribution on the passive flank. The qualitative spatial distribution is similar to COL despite the difference in thermocouple positioning. C1L (Figure 10b) and C2L (Figure 10d), with the shorter distances between the impingement and the meshing zones, result in more uniform axial distributions of HTC on the active flank. The increase in uniformity is in line with the expected order of influence in relation to the distance between impingement and meshing zones. The reason behind the increasing uniformity with decreasing distance could be the spreading of the oil film by the meshing teeth before either the oil film gets flung-off by the centrifugal forces acting upon it or the heat transfer approaches a saturation state, where the temperature difference between the oil film and the tooth surface tends towards zero.

The proposed cooling setups found in the literature [15, 20] employ oil jets impinging on the disengaging side of the meshing teeth for better cooling performance. The present work reveals that an impingement right before the meshing would result in a slightly more optimal cooling of the gear teeth. Even if the mean HTC deviation between C1L and C1R can be attributed to the rotational direction difference as discussed before, the axial distribution of HTC on the active flank is more uniform with C1L. This ensures that it is less likely to have local hotspots on the active flank of the gear tooth. However, it should be noted that the meshing in the real-world application might result in a different or increased influence since the transmitted high loads and finer tolerances of the gears could lead to thinner oil films and more uniform spreading of the oil film on the tooth surface.

## 5.0 CONCLUSION

The experimental setup is modified in order to investigate the cooling of meshing gears with the inclined impingement cooling method. Meshing results in extremely high gear temperatures, especially at high rotational speeds. This temperature increase is not explicable with a change in the heat transfer characteristics of the jet impingement. A loss analysis is carried out to quantify the individual loss components that could lead to the observed effect. A variation of braking power rules out a possible influence of friction. It is shown that windage and load-independent bearing losses, as well as oil momentum variation losses, can be very accurately determined using the derived fitting functions and calculation methods from the literature. The calculated losses are utilized to determine

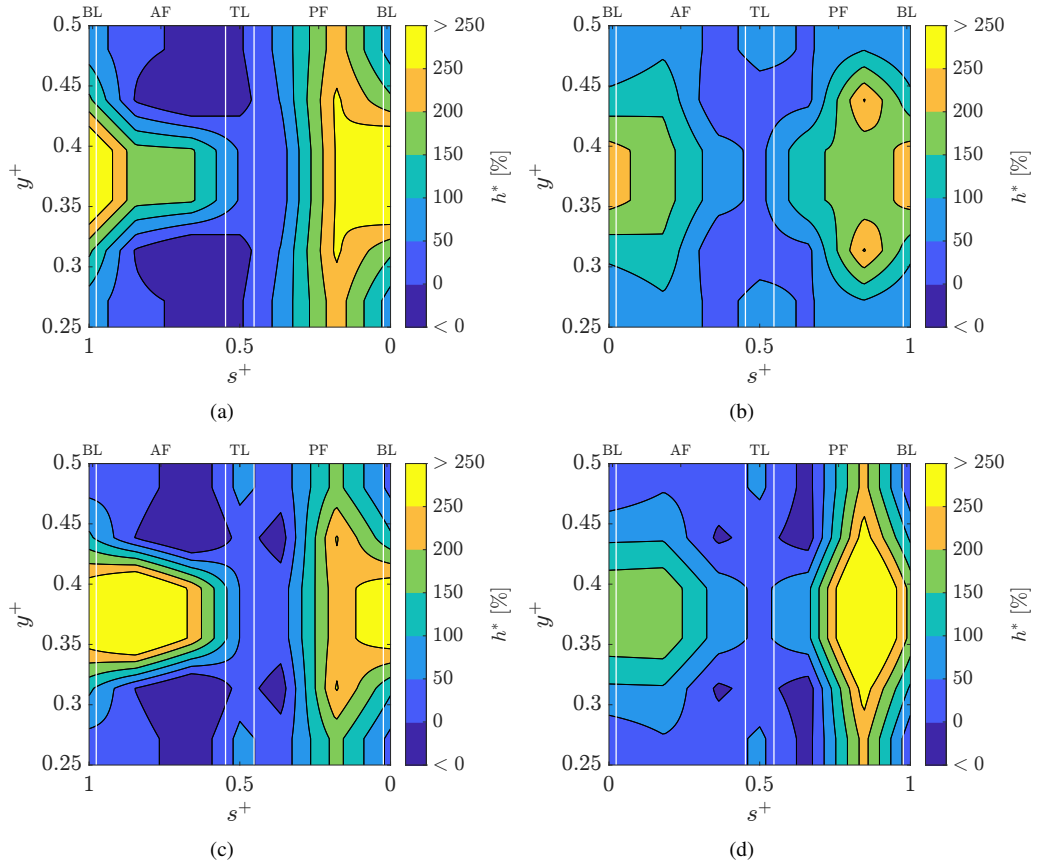


Figure 10: Heat transfer map with  $\dot{V}_{oil} = 3.2l/min$ ,  $\omega = 2000$  RPM and configuration C1R in (a), C1L in (b), C2R in (c) and C2L in (d).

the trapping losses in the meshing configuration measurements, assuming that a superposition of the windage and bearing losses is valid. Determined trapping losses correlate strongly with the inexplicable increase in the heat transfer coefficient (HTC).

The measurements at lower rotational speed with relatively low trapping losses are selected to investigate the influence of meshing on the heat transfer. The mean HTC difference between meshing and non-meshing configurations is not significant. Deviations from the non-meshing configuration can be attributed to the trapping losses. A dependence of the mean HTC on the rotational direction is suspected. Measurements with a non-meshing and clockwise rotating gear are required for further investigation. A correlation between the mean HTC and the distance between impingement and meshing zones is not observed. Nevertheless, a decrease in this distance leads to a more uniform HTC distribution on the active flank, rendering the impingement on the engaging side of the meshing gears more preferable contrary to the proposed cooling setups in the literature.

Further research is required for a correction of the trapping losses in order to enable an investigation of heat transfer at high rotational speeds and increase the accuracy of the results presented within this work. If also at higher rotational speeds there is no apparent effect of meshing on the mean HTC, measurements without meshing can be utilized to investigate the heat transfer characteristics more in detail since these are easier to conduct, more accurate, and more robust. Furthermore, measurements with into-mesh and out-of-mesh impingement methods would be beneficial to enable a direct comparison of the established cooling strategies.

## ACKNOWLEDGEMENTS

The funding for the research activities of this study was provided by the Bundesministerium für Wirtschaft und Klimaschutz (BMWK) and Rolls-Royce Deutschland Ltd. and

Co. KG within the framework of Luftfahrtforschungsprogramm 5 (Project No. 20T1729). The authors gratefully acknowledge this financial support and are solely responsible for the content.

## REFERENCES

- [1] ARIURA, Y., UENO, T., SUNAGA, T., AND SUNAMOTO, S. The lubricant churning loss in spur gear systems. *Bulletin of JSME* 16, 95 (1973), 881–892.
- [2] AYAN, E., VON PLEHWE, F. C., KELLER, M. C., KROMER, C., SCHWITZKE, C., AND BAUER, H.-J. Experimental determination of heat transfer coefficient on impingement cooled gear flanks: Validation of the evaluation method. *Journal of Turbomachinery* 144, 8 (2022), 229.
- [3] DAI, Y., JIA, J., OUYANG, B., AND BIAN, J. Determination of an optimal oil jet nozzle layout for helical gear lubrication: Mathematical modeling, numerical simulation, and experimental validation. *Complexity* 2020 (2020), 1–18.
- [4] DEWINTER, A., AND BLOK, H. Fling-off cooling of gear teeth. *Journal of Engineering for Industry* 96, 1 (1974), 60.
- [5] FERNANDES, C. M., ROCHA, D. M., MARTINS, R. C., MAGALHÃES, L., AND SEABRA, J. H. Finite element method model to predict bulk and flash temperatures on polymer gears. *Tribology International* 120 (2018), 255–268.
- [6] FONDELLI, T., ANDREINI, A., DA SOGHE, R., FACCHINI, B., AND CIPOLLA, L. Numerical simulation of oil jet lubrication for high speed gears. *International Journal of Aerospace Engineering* 2015, 3 (2015), 1–13.
- [7] FONDELLI, T., MASSINI, D., ANDREINI, A., FACCHINI, B., AND LEONARDI, F. Three-dimensional cfd analysis of meshing losses in a spur gear pair. In *Volume 5B: Heat Transfer* (2018), American Society of Mechanical Engineers.
- [8] HANDSCHUH, R. Effect of lubricant jet location on spiral bevel gear operating temperatures. NASA Technical Memorandum 105656, Lewis Research Center, Cleveland, Ohio, 1992.
- [9] KELLER, M. C., KROMER, C., CORDES, L., SCHWITZKE, C., AND BAUER, H.-J. Cfd study of oil-jet gear interaction flow phenomena in spur gears. *The Aeronautical Journal* 124, 1279 (2020), 1301–1317.
- [10] LEONI, P. *Hochleistungsgetriebe mit getrennter Schmierung und Kühlung*. Dissertation, Universität Stuttgart, Stuttgart, 1991.
- [11] LI, W., AND TIAN, J. Unsteady-state temperature field and sensitivity analysis of gear transmission. *Tribology International* 116 (2017), 229–243.
- [12] LONG, H., LORD, A. A., GETHIN, D. T., AND ROYLANCE, B. J. Operating temperatures of oil-lubricated medium-speed gears: Numerical models and experimental results. *Proceedings of the Institution of Mechanical Engineers, Part G: Journal of Aerospace Engineering* 217, 2 (2003), 87–106.
- [13] MASSINI, D., FONDELLI, T., FACCHINI, B., TARCHI, L., AND LEONARDI, F. Experimental investigation on power losses due to oil jet lubrication in high speed gearing systems. In *Volume 5B: Heat Transfer* (2017), American Society of Mechanical Engineers.
- [14] MASSINI, D., FONDELLI, T., FACCHINI, B., TARCHI, L., AND LEONARDI, F. Windage losses of a meshing gear pair measured at different working conditions. In *Volume 5B: Heat Transfer* (2018), American Society of Mechanical Engineers.
- [15] MCCAIN, J. W., AND ALSANDOR, E. Analytical aspects of gear lubrication on the disengaging side. *A S L E Transactions* 9, 2 (1966), 202–211.
- [16] NIEMANN, G., AND WINTER, H. *Getriebe allgemein, Zahnradgetriebe - Grundlagen, Stirnradgetriebe*, vol. Bd. 2 of *Maschinenelemente*. Springer, Berlin, 1983.
- [17] PATIR, N., AND CHENG, H. S. Prediction of the bulk temperature in spur gears based on finite element temperature analysis. *A S L E Transactions* 22, 1 (1979), 25–36.

- 
- [18] RUZEK, M., MARCHESSE, Y., VILLE, F., AND VELEX, P. Windage power loss reductions in high-speed gear pairs. *Forschung im Ingenieurwesen* 83, 3 (2019), 387–392.
  - [19] SCHOBER, H. *Einspritzschmierung bei Zahnradgetrieben*. Dissertation, Universität Stuttgart, Stuttgart, 1983.
  - [20] TOWNSEND, D. P. Lubrication and cooling for high speed gears. NASA Technical Memorandum 101430, Lewis Research Center, Cleveland, Ohio, 1985.
  - [21] TOWNSEND, D. P., AND AKIN, L. S. Gear lubrication and cooling experiment and analysis. *J Mech Design* 103, 4 (1981), 219–226.
  - [22] VON PLEHWE, F. C., SCHWITZKE, C., AND BAUER, H. J. Heat transfer coefficient distribution on oil injection cooled gears: Experimental method, uncertainty and results. *J Tribol* 143, 9 (2021). Published Online: January 8, 2021.